

Article

GAN-based Differential Private Image Privacy Protection Framework for Internet of Multimedia Things

Version November 9, 2020 submitted to Journal Not Specified

Abstract: With the development of Internet of Multimedia Things (IoMT), more and more image data is collected by various multimedia devices, such as smart phones, cameras, drones. These massive amount of images are widely used in each field of IoMT, which presents substantial challenges for privacy preservation. In this paper, we propose a new image privacy protection framework, with an effort to protect the sensitive personal information contained in images collected by IoMT devices. We aim to use deep neural network techniques to identify the privacy-sensitive content in images, and then protect it with synthetic content generated by generative adversarial networks (GANs) with differential privacy (DP). Our experimental results show that the proposed framework can effectively protect users' privacy while maintaining image utility.

Keywords: Internet of Multimedia Things (IoMT), image privacy, object detection, deep learning, generative adversarial network, differential privacy

1. Introduction

The recent advances in multimedia-recording devices, such as phones, cameras, drones, and other type of sensors, have greatly facilitated the collection of multimedia data, especially in the form of images and videos. In such an era of IoMT, a massive amount of images are widely used, not only by social network personal users but also by government and companies. Image data is the most representative type of data in IoMT data collection, which contain sensitive information that might be used to dig personal information. Data mining attacks on images can easily cause privacy leakage, which can cause serious consequences. The issue of privacy leakage has been paid attention by the public in recent years, which has aroused public concern about this issue. Moreover, privacy issues are no longer just personal concerns as many countries have launched privacy acts and laws. For example, the European General Data Protection Regulation (GDPR) took effect on 25 May 2018 [1]. Any violations of the regulation will trigger heavy fines and penalties. GDPR emphasizes the protection of "personal data", interpreting as "any information relating to an identified or identifiable natural person ('data subject'); an identifiable natural person is one who can be identified, directly or indirectly, in particular by reference to an identifier such as a name, an identification number, location data, an online identifier or to one or more factors specific to the physical, physiological, genetic, mental, economic, cultural or social identity of that natural person" [2]. According to this definition, images include a variety of personal identifiers such as people's faces, text and license plates. Therefore, effective image privacy protection techniques are in urgent need.

The research community has seen some effort in image privacy protection. The early works mostly focus on the access control of the data, i.e., privacy protection by safeguarding against unauthorized access. This can be achieved through setting preferences of users [3] [4] or tags control [5] [6]. However, these methods cannot be applied to the scenarios where the images are shared openly, but some sensitive information needs to be concealed. For example, in the "Google Street View" application,

we have full access to photos showing the streets while people's faces and other personal identifiers have been obfuscated, e.g. by blurring. To achieve this, the privacy protection methods need to detect, and then cover/remove/replace sensitive content in images. There are some recent research in this direction [7] [8] [9] [10] [11] [12] [13] [14]. For example, Viola et al. [7] used a sliding window detector to identify and blur the license plates in Google Street View images. Yu et al. [9] used a deep multi-task learning algorithm to detect privacy-sensitive objects and provide simple protection by blurring. Overall, most of the existing work performs personal data detection as the first step of privacy protection. While on the protection part, it mostly relies on simple approaches such as blurring or pixelation. Consequently, the image utility suffers to a considerable extent. It not only makes the images look unnatural, but also makes the person who looks at the image aware that the obfuscated part is private. Moreover, such a protection mechanism is powerless in facing the emerging attacks based on advanced deep neural networks. For example, Mcpherson et al. [15] use artificial neural networks to recover hidden information from images protected by pixelation, blurring and P3. And the method obtained good results on different data sets, MINIST 80%, CIFAR-10 75%, ATT dataset 95%, FaceScurb 57%.

Moreover, the existing methods are almost discussing single object protection, such as face or text. However, most images that require privacy protection have multiple objects that need to be protected (For example, in street view images, human faces and license plates need to be protected at the same time).

Current methods are unable to find a way to quantify the tradeoff between image usability and privacy protection. To tackle this, we use DP to control the image private objects generation to mitigate privacy threats.

To overcome these obstacles, we propose the a three-stage frameworks for image privacy protection in this paper. The framework consists of three steps: 1) privacy-sensitive content detection and position extraction powered by a deep Convolutional Neural Network: We use CNN networks to detect various objects in images and classifying objects into private and non-private ones; 2) real private objects projecting into latent space: We use generative adversarial networks (GANs) to projecting the real private objects of the images into latent space and get the corresponding latent vector ω . 3) private content generation controlled by DP (de-identification): We use Laplace noise into the latent vector ω and generated de-identification content. Finally, replace the originally private objects with the synthetic ones to protect users' privacy.

In order to evaluate the performance of our proposed framework, we have conducted extensive experiments on a real-world image data set collected by cameras of IoMT, and investigated two types of personal identifier related data: license plate and face. We choose these two types of objects as they represent the two most significant categories of personal identifiers in images.

In summary, the contributions of this paper are as follows:

- We propose an image privacy protection framework that can protect the privacy in the IoMT's image.
- We propose a GAN-based method to generate the replacement content for private objects in the images.
- We use differential privacy methods to disturb generation to quantify the tradeoff between image usability and privacy protection.

The remaining of the paper is organized as follows. Section 2 reviews the related work. Section 3 give the definition and foundation of the methods. Section 4 presents our framework on multimedia privacy protection based on Mask-RCNN and synthetic content generation using GANs. Section 5 shows the experimental results of our framework for multi-object privacy protection (street view scenarios). Section 6 concludes the paper and outlines the future work.

83 2. RELATED WORK

84 Privacy protection, in general, has been extensively studied in recent years. Among all the
85 researches, differential privacy (DP) has attracted the most attentions and applied to different
86 application. Therefore, in this section, we will review the most relevant research works on image
87 privacy and the related fundamental deep learning researches, including: (1) image privacy issue and
88 protection; (2) deep learning and object detection of the images; (3) the content generation; (4) and
89 privacy protection.

90 2.1. Image Privacy Issue and Protection

91 The image privacy issue first attracted people's attention along with the booming of social
92 networks developing. The proliferation of social networks generated massive photos flooding on the
93 internet that contains sensitive information. For example, Pesce et al. [16] use photo tags to attack
94 users and get their privacy. The image privacy issue becomes more server with the widely spread of
95 facial recognition systems, as people start to worry that their faces might be used by organizations for
96 profiling or social control.

97 To combat the image privacy attack, the previous mainstream method is using access control
98 on sensitive contents. Mannan et al. [3] use Instant Messaging (IM) networks to control personal
99 web content sharing. Vyas et al. [4] use annotation data to predict the privacy preferences of users
100 and control the shared content. Wang et al. [5] studied privacy control on Facebook. Moreover,
101 Squicciarini et al. [6] proposed collaborative privacy management that can let users collaborative
102 control their photos. Similarly, to deal with the privacy issue in facial recognition systems, the current
103 countermeasure is simply banning [17]. The access control-based method has several limitations. It
104 only gives "Yes" or "No" options for the use of images, while we need to use part of the information in
105 applications such as Google Street View. And it can not automate protect privacy based on the privacy
106 information of the image itself, requiring human participation.

107 Some more recent image privacy researches focus on the inherently implicit information of the
108 photos. Tonge et al. [8] explore learning models that can automatically classify the private or public
109 parts in an image by using Deep Neural Networks. Yu et al. [9] create a new tool called "iPrivacy" that
110 uses a deep learning algorithm to detect the privacy-sensitive objects. Yu's work can detect the privacy
111 parts of photos, but in the step of privacy protection, they just use blur to protect privacy which is
112 not good looking. More than blurring, Uittenbogaard's work [10] set a framework that automatically
113 removes moving objects. However, there are two limitations, one only for moving objects and the
114 other for missing partial information in the image. Liu's work [11] proposes a novel Stealth algorithm,
115 which makes the automatic detector can not detect the objects in an image. However, human beings
116 can easily get privacy information from the image.

117 Our framework is a further advancement compared with the researches mentioned above. It can
118 identify the privacy part of the photos in the pixel level. Then it will generate the target replacement
119 content based on the privacy content, not just using mosaic, blurring or removing to protect privacy.
120 Our framework can protect privacy information from both human and machine.

121 2.2. Deep Learning-based Image Object Detection and Segmentation

122 Object detection and semantic segmentation technologies have been advancing rapidly in recent
123 years. In the beginning, Girshick et al. [18] use high-capacity convolutional neural networks (CNNs)
124 to bottom-up region proposals, which called R-CNN. This algorithm improves the mean average
125 precision (mAP). In 2015, Hariharan et al. [19] define the hypercolumn at a pixel as the vector of
126 activations of all CNN units above that pixel to improve the result of the experiment. After that, a
127 large part of the research works are based on the Fast R-CNN [20] [21] and Fully Convolution Network
128 (FCN) [22]. The disadvantage of Faster R-CNN is that it cannot deal with pixel-to-pixel alignment
129 between the inputs and outputs of the network. To solve this problem, He et al. proposed a method

130 called Mask R-CNN [23] that extends the Fast R-CNN by adding predicting segmentation masks on
131 each Region of Interest (RoI) to get the results. As our goal is to find the privacy part of the images, so
132 we choose to use the Mask R-CNN to get the instance segmentation results that can be used as the
133 basis for the follow-up privacy content detection and positioning. To obtain good results for our use
134 case, we need to re-train the network using our image dataset that includes more privacy sensitive
135 contents.

136 2.3. GAN-based Content Generation

137 Preliminary ways for image privacy content protection include blurring, deletion, etc. In this paper,
138 we use the replacement of content to protect privacy, i.e. generating content without identification
139 information to replace the privacy content in the images. Traditional content generation methods
140 such as [24] [25] [26] [27] just fill the pixels by matching and pasting based on the low-level features
141 in the images. The effect is not very satisfactory as they often produce the failure contents and the
142 results obtained are also not good. In 2014, Goodfellow proposed a new framework called GAN [28]
143 can synthesize new content by training the models. Following the GAN-based method, the latest
144 GAN-based generation content generation technology can generate very realistic content, such as faces,
145 cats, dogs, even Airbnb rooms [29] [30] [31] [32]. In our framework, we use StyleGAN [33] to generate
146 the replacement content. The StyleGAN can generate content which is not much different from the
147 real image. The image content generated by StyleGAN does not exist in real life and these contents can
148 avoid copyright disputes. With the replacement of the generated content, the privacy of the images
149 can be protected.

150 2.4. Privacy Protection

151 In the traditional privacy protection technology, one of the most common method is data
152 encryption, which has high security. However directly encrypted and decrypted on large-scale data
153 such as image sets will consume a lot of computing resources. Another privacy protection methods is
154 anonymity privacy protection technology. In 2002, Sweeney et al. proposed k-Anonymity[34] method
155 to protect privacy. Machanavajjhala proposed l-Diversity[35] to address the limitations of k-Anonymity,
156 and Li et al. introduced t-Closeness[36]. However, with the development of attack technology, attackers
157 can use data mining, machine learning, background knowledge attack, and big data analysis to obtain
158 enough useful information of the privacy. To solve this problem, Dwork[37] proposed the concept of
159 differential privacy which has a solid mathematical theoretical foundation. Once differential privacy is
160 proposed, it has attracted attention in the field of privacy protection, and various privacy protection
161 algorithms based on differential privacy have been proposed. In this paper, we propose a new image
162 privacy protection method based on the differential privacy method combined with GANs. Take
163 advantage of the controllability of differential privacy, our method can protect the privacy of IoMT
164 images with high controllability.

165 3. Preliminaries

166 3.1. Privacy Protection and Image Utility

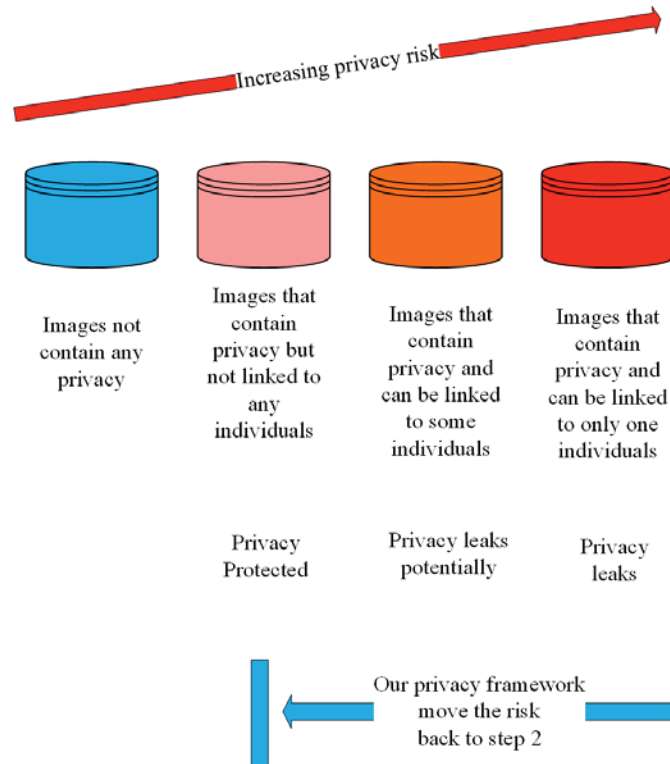


Figure 1. The four levels of image privacy risks.

167 In this part, we discuss the image privacy protection and image utility. Firstly, the different
 168 levels of image privacy risk are shown in Fig. 1. On the left is images that do not contain any
 169 private information (such as a landscape photograph) and the risk of privacy leakage is zero. On
 170 the right is images that contain private information and can be linked to specific individuals which
 171 violates individuals' privacy directly. Between the two extreme cases are images that contain private
 172 information but might not leak individuals privacy. Our goal is to propose a framework to reduce the
 173 risk of privacy leak from Level 3/4 back to Level 2 in Fig. 1. It means that we can protect privacy in
 174 images so that they cannot be linked to any individual.

175 However, the strength of privacy protection will affect the utility of images. The common methods
 176 such as mosaic and blur, might reduce the utility of the image while image processing. The greater
 177 privacy protection, will result in lower utility of images, example shown in Fig. 2. Although mosaic or
 178 blur methods protect the privacy, it reduces the readability and usability of the images. It also make
 179 images sharing pointless. In our image privacy protection framework, we found an effective way to
 180 compromise between privacy protection and image utility.



Figure 2. The privacy and utility.

181 3.2. Formulation of Image De-Identification

182 We now formally define the problem of image de-identification. This part help us to define the
183 problem we need to deal with and build the foundation for following discussions.

184 **Definition 3.1. (Image).** An image is a matrix I of m columns, n rows and c channels. The c
185 channels usually is 3 in common color space such as RGB and YUV. Each cell in matrix I contains a
186 coding which ranging from 0 to 255. Image should contains multi private objects such as face or text.

187
188 **Definition 3.2. (Object sets).** An object set is a set of M objects images contained in image matrix
189 $I: O_i : i = 1, 2, \dots, M$.

190
191 **Definition 3.3. (Privacy object sets).** A private object set is a set of N objects images contained in
192 image matrix $I: P_i : i = 1, 2, \dots, N$. Which $P_i \in O_i$ and $N \leq M$.

193
Definition 3.4. (Privacy Object De-Identification Function). Let P and P_d be a private object set
and de-identification object set.

$$f : P \rightarrow P_d \quad (1)$$

194 f is defined de-identification function for each P to remove their identity.

195
Definition 3.5. (Image De-Identification). Given image matrix I and de-identification function
 f , for each private object $P_i \in O_i$:

$$I_d = f(I) \quad (2)$$

196 which we can use de-identification function to get an image matrix I_d not contain privacy.

197 3.3. Differential Privacy

Definition 3.6. (Differential Privacy). The formal definition of DP is given by (3):

$$Pr[K(D_1) \in S] \leq exp(\epsilon) \times Pr[K(D_2) \in S] \quad (3)$$

Definition 3.7. (The Sensitivity of Differential Privacy). The sensitivity of DP is defined in (4),
which determines how much perturbation is required in the DP mechanism.

$$\Delta f = \max_{D_1, D_2} ||f(D_1) - f(D_2)||_1 \quad (4)$$

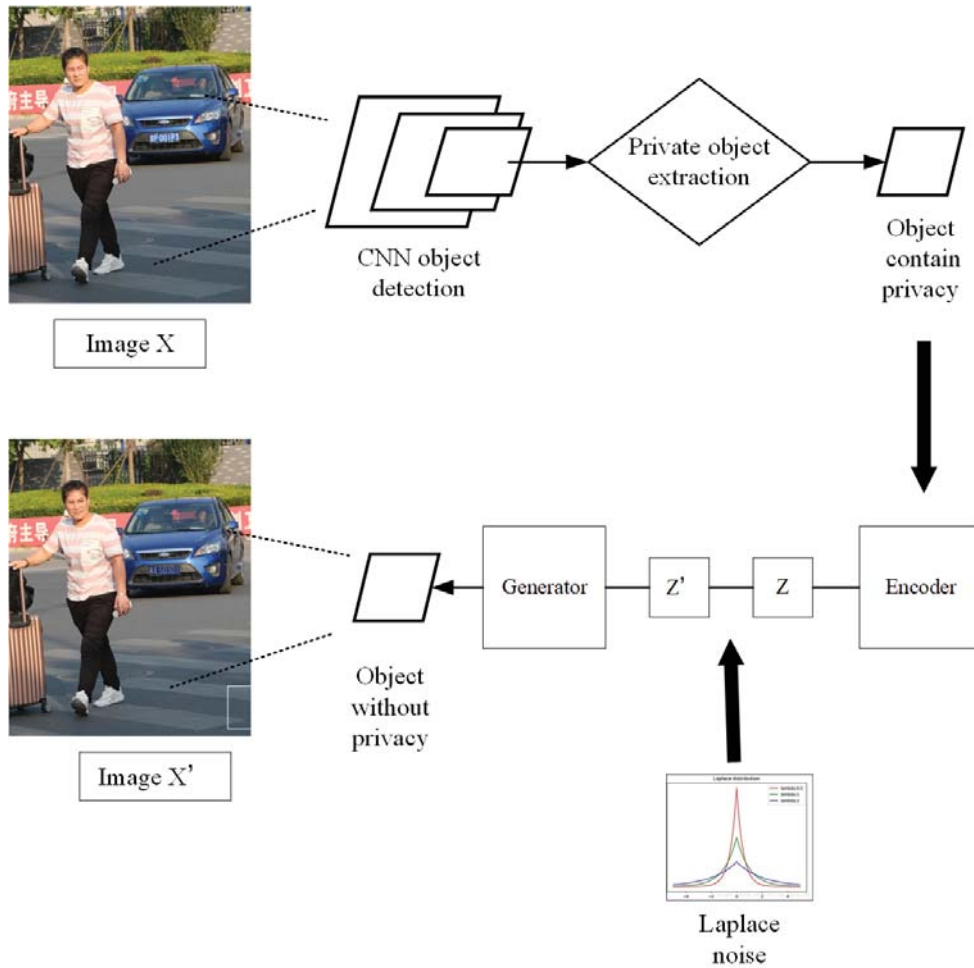
198 **4. Image De-identification Framework**

Figure 3. The diagram of the proposed image de-identification (DE-ID) framework.

199 In order to achieve the above goal of image privacy protection, we propose an image
 200 de-identification framework consists of three steps: (a) objects detection and private objects extraction;
 201 (b) de-identification content generation; and (c) content replacement and image privacy protection.

202 Fig. 3 shows the diagram of the framework. The original image *X* contains privacy information
 203 such as face and car plate. It is first input into a CNN to identify and extract the private objects in the
 204 image. Then we transform the extracted private objects into latent space and use differential privacy
 205 to control the de-identified content generation. Finally, we get a de-identified image *X'*, i.e., image
 206 without any sensitive information. In the following part of this section, we will explain the framework
 207 in details.

208 4.1. Step-I: objects detection and private objects extraction

209 To protect the privacy of an image, it is necessary to detect the sensitive privacy zone in the
 210 image. We use two steps to achieve this target. First, all objects in the image are detected, and then the
 211 included private objects are extracted.

212 4.1.1. Objects detection

213 The state-of-the-art object detection algorithm Mask-RCNN is used to detect the objects in the
 214 image.

215 For an image I , the ROI (region of interest) vector X_{roi} of each object O_i can be detected by $R(\cdot)$:

$$\begin{aligned} X_{roi} &= R(I) = (P|E_p) \\ &= \left(\begin{array}{cccc|cccc} x_1 & y_1 & w_1 & h_1 & p_{11} & p_{12} & \cdots & p_{1m} \\ x_2 & y_2 & w_2 & h_2 & p_{21} & p_{22} & \cdots & p_{2m} \\ \vdots & \vdots & \vdots & \vdots & \vdots & \vdots & \vdots & \vdots \\ x_n & y_n & w_n & h_n & p_{n1} & p_{n2} & \cdots & p_{nm} \end{array} \right), \end{aligned} \quad (5)$$

216 where $P_n = (x_n, y_n, w_n, h_n)$ is position vector including the information of up left corner coordinate
217 (x_i, y_i) , width w_i and height h_i of object O_i . The probability of objects noted as E_p , the E_{pi} is the
218 probability of Object O_i belonging to the m th class (there are m class objects in the image I).

In (5), we choose the maximum probability c_i in each E_{pi} , so the output of the object detection shown as blew:

$$X_c = (P|C_p) = \left(\begin{array}{cccc|c} x_{p1} & y_{p1} & w_{p1} & h_{p1} & c_1 \\ x_{p2} & y_{p2} & w_{p2} & h_{p2} & c_2 \\ \vdots & \vdots & \vdots & \vdots & \vdots \\ x_{pn} & y_{pn} & w_{pn} & h_{pn} & c_n \end{array} \right), \quad (6)$$

219 where $\forall i \in (1, n)$:

$$220 \quad c_i = \begin{cases} \arg \max(p_{ij}), 1 \leq j \leq m; \text{ if } \max(p_{ij}) > \delta \\ c_{bg}, \text{ if } \max(p_{ij}) \leq \delta \end{cases}$$

221 In Mask-RCNN, if the maximum probability is smaller than a threshold δ , this object will be
222 treated as the background class, otherwise the object belongs to class i .

223 4.1.2. Private Objects extraction

224 After getting the objects' information and position, we set a classifier to classify the objects as
225 either private of non-private. In our the street View experiment scene, the private objects can be human
226 face, car plates, etc. The non-private objects can be as background, tree, traffic lights.

227 The extraction process is finished by $D(\cdot)$ accordingly as shown in (7).

$$\begin{aligned} D(X_c) &= D \left(\begin{array}{cccc|c} x_{p1} & y_{p1} & w_{p1} & h_{p1} & c_{p1} \\ \vdots & \vdots & \vdots & \vdots & \vdots \\ x_{p\alpha} & y_{p\alpha} & w_{p\alpha} & h_{p\alpha} & c_{p\alpha} \\ \hline x_{np1} & y_{np1} & w_{np1} & h_{np1} & c_{np1} \\ \vdots & \vdots & \vdots & \vdots & \vdots \\ x_{np\beta} & y_{np\beta} & w_{np\beta} & h_{np\beta} & c_{np\beta} \end{array} \right) \\ &= \left(\begin{array}{cccc|c} x_{p1} & y_{p1} & w_{p1} & h_{p1} & c_{p1} \\ x_{p2} & y_{p2} & w_{p2} & h_{p2} & c_{p2} \\ \vdots & \vdots & \vdots & \vdots & \vdots \\ x_{p\alpha} & y_{p\alpha} & w_{p\alpha} & h_{p\alpha} & c_{p\alpha} \end{array} \right). \end{aligned} \quad (7)$$

228 So we got the private objects' position, class, and pixel information. The private objects'
229 information is represented as follows:

$$X_i = D(P|C_p) = \left(\begin{array}{cccc|c} x_{p1} & y_{p1} & w_{p1} & h_{p1} & c_{p1} \\ x_{p2} & y_{p2} & w_{p2} & h_{p2} & c_{p2} \\ \vdots & \vdots & \vdots & \vdots & \vdots \\ x_{p\alpha} & y_{p\alpha} & w_{p\alpha} & h_{p\alpha} & c_{p\alpha} \end{array} \right) \quad (8)$$

230 4.2. STEP-II: De-identification content generation

231 In the second step, we use a content generator $G(\cdot)$ and the differential privacy method to generate
232 the de-identification content. The algorithm shown as below:

Algorithm 1: Image De-identification Content Generation

Input: The original image $I \in \mathbb{R}^{n \times m \times 3}$ to de-identify; A pre-trained generator $G(\cdot)$.
Output: The de-identified image I_{de} optimized via $G(\cdot)$
Initialize latent vector ω , differential privacy Laplace noise with Δf and ϵ ;
while not converged **do**
| $I \simeq I' = G(\omega^*)$;
end
 $I_{de} = G(\omega^* + Lap(\frac{\Delta f}{\epsilon}))$;

Firstly, we find the latent vector ω^* of each input image I . Initialize a latent vector ω and search for a optimized vector ω^* minimizes the loss function (9) that measures the similarity between the private object image and image generated by latent vector ω^* . This step enables the image editable.

$$\omega^* = \arg \min_{\omega} \mathcal{L}_{percept}(G(\omega^*), I) + \frac{\lambda_{mse}}{N} \|G(\omega^*) - I\|_2^2, \quad (9)$$

233 where image $I \in \mathbb{R}^{n \times m \times 3}$ is the input privacy image. $G(\cdot)$ is the pre-trained generator, N is the number
234 of scalars in the image, ω is the latent code to optimize, $\lambda_{mse} = 1$.

235 Secondly, after we got latent vector ω^* of each private objects, we put the Laplace noise on latent
236 vector ω^* . Then put the new latent vector into the generator $G(\cdot)$ and got the de-identify content.

$$I_{de} = G(\omega^* + Lap(\frac{\Delta f}{\epsilon})) \quad (10)$$

In equation (10), we used the DP criterion to protect the sensitivity information of the image. The Laplace mechanism was used. Generally speaking, the Laplace mechanism adds a controlled Laplace noise to a query result before returning it to the user. Here, the Laplace noise is sampled from a Laplace distribution, which is showed in (11).

$$Lap(x) = \frac{1}{2b} \exp(-\frac{|x|}{b}) \quad (11)$$

To sum up, the Laplace mechanism can be summarized as

$$M(D) = f(D) + Lap(\frac{\Delta f}{\epsilon}) \quad (12)$$

237 The Laplace mechanism in (12) indicates that the size of the Laplace noise is related to the
238 sensitivity of query f and the privacy budget ϵ . A larger sensitivity leads to a higher noise. In our
239 method, we use privacy budget ϵ to control our GAN generator to generate the synthetic de-identify
240 content.

241 4.3. STEP-III: De-identification content replacement

242 After de-identification contents generated, we use the generated content to replace the original
243 private object images. The algorithm is shown in ??.

244 Finally, we get the de-identified image I_{de} .

Algorithm 2: Image Protected by de-identification content swapping

Input: The original image $I \in \mathbb{R}^{n \times m \times 3}$ contains private content $X_i, i = 1, 2, \dots, N$;
de-identified contents in the image: $X_i^{de}, i = 1, 2, \dots, N$

Output: The protected image $I_d \in \mathbb{R}^{n \times m \times 3}$

for each X_i^{de} **in** X^{de} **do**

$X \xleftarrow{\text{swapping}} X_i^{de}$

end

$I_d = I(X \xleftarrow{\text{swapping}} X^{de})$

245 **5. Experiments and Discussions**

246 5.1. Experiment Setup

247 First of all, we set up an experiment database contains amount of street view images collected by
248 IoMT technology. The street view images contains human faces, car license plates, road signs, traffic
249 lights and more. In these images, the sensitive private information are human faces and car license
250 plates. In our test database, the human faces and car plates are the private objects, and the road sign,
251 the traffic light and background are the non-private objects. We use the camera to collect over 4000
252 typical street view images as the test database.

253 5.2. Performance Evaluation Metrics

254 5.2.1. Privacy metrics

255 **Confidence Score.** In the privacy protection metric for human face, we use the open-source "face
256 recognition" platform to evaluate the confidence in face privacy. This platform was built using dlib's
257 state-of-the-art face recognition which was built with deep learning. The model has an accuracy of
258 99.38% on the Labeled Faces in the Wild benchmark. The output of the platform is the facial distance
259 between each unrecognized face and the recognized face. By setting the corresponding threshold, the
260 distance metric can judge whether the face is protected. This means after the face photo is processed
261 by our method, whether the general third-party platform still considers the same person. The default
262 threshold is 0.3.

263 **Distance.** In the privacy protection metric for the car license plate, due to the license plate is a set
264 of characters, we believe that the distance between the original license plate and the processed license
265 plate is the privacy metric. In the experiment, we set the threshold of the car license plate for 3. This
266 means that the sensitive information of the license plates is protected when the distance is greater than
267 3.

268 5.2.2. Image utility metrics

269 The quantitative judgment is necessary for the degree of modification between the original image
270 and the protected image. So we use several metrics to calculate the degree of modification, these
271 metrics include L_0 , L_2 , ALD_p , Structural similarity index(SSIM), and difference value hash(Dhash).
272 Deciding there are two images: processed image X^a and original image X , the utility image metrics
273 are:

The L_0 calculate the number of pixels changed.

$$L_0 = \text{num}(X^a, X) \quad (13)$$

274 where num is calculated the number of pixels changed between X^a and X .

The L_2 calculate Euclidean distance between the original image and protected image.

$$L_2 = \|X^a - X\|_2 = \sqrt{\sum_{i=1}^N (X_i^a - X_i)^2} \quad (14)$$

The ALD calculate the average L distance between the images.

$$ALD_p = \frac{1}{n} \sum_{i=1}^n \frac{\|X_i^a - X_i\|_p}{\|X_i\|_p} \quad (15)$$

The SSIM is the common method to evaluate the similarity between the original image and the protected image.

$$SSIM(X^a, X) = \frac{1}{n} \sum_{i=1}^n SSIM(X_i^a, X_i) \quad (16)$$

The Dhash use the difference hash to evaluate the degree of modification which value is the smaller the better.

$$Dhash(X^a, X) = hash(X^a) - hash(X) \quad (17)$$

275 5.3. Street view image protection

276 5.3.1. Human face privacy protection

277 Human face is the most sensitivity information of the IoMT images, which can straight leak
 278 personal identification. Therefore, we use our method to protect the human face privacy in the street
 279 view experimental scene. Firstly, we use Mask-RCNN to extra the human face images I from the
 280 experimental street view images. Secondly, initialize a latent vector ω and use the loss function (18) to
 281 find the latent vector ω^* of human face I . The algorithm to find the latent vector ω^* was shown in
 282 algorithm (3).

Algorithm 3: Human face Image Projecting into Latent Space

Input: A human face image $I \in \mathfrak{R}^{n \times m \times 3}$ to project; a pre-trained generator $G(\cdot)$

Output: The latent code ω^* and the projected image $G(\omega^*)$ optimized via F'

Initialize latent code $\omega^* = \omega$

283

while not converged **do**

| $L \leftarrow L_{percept}(G(\omega^*), I) + \frac{\lambda}{N} \|G(\omega^*) - I\|_2^2$
 | $\omega^* \leftarrow \omega^* - \eta F'(L)$

end

In algorithm (3), the loss function was show in (18).

$$\omega^* = \min_{\omega} L_{percept}(G(\omega^*), I) + \frac{\lambda_{mse}}{N} \|G(\omega^*) - I\|_2^2 \quad (18)$$

where image $I \in \mathfrak{R}^{n \times m \times 3}$ is the input privacy image. $G(\cdot)$ is the pre-trained generator, N is the number of scalars in the image, ω is the latent code to optimize, $\lambda_{mse} = 1$. For the loss term $L_{percept}$, shows as below:

$$L_{percept} I_1, I_2 = \sum_{j=1}^4 \frac{\lambda_j}{N_j} \|F_j(I_1) - F_j(I_2)\|_2^2 \quad (19)$$

284

where $I_1, I_2 \in \mathfrak{R}^{n \times m \times 3}$ are the input images, F_j is the feature output of VGG-16 layers conv1_1, conv1_2, conv3_2, conv4_2. N_j is the number of scalars in the j th layer output, $\lambda_j = 1$ for all js are empirically obtained for good performance.

285
286

287 Fig. 4 is an example of the original human face image and the human face generated by GAN
 288 with no modify.

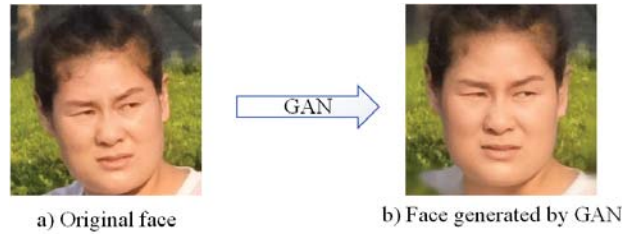


Figure 4. The original face image projecting into StyleGAN

Thirdly, put the Laplace noise on the latent vector ω^* and use the generator $G(\cdot)$ to generate the de-identify human face image.

$$I_{de} = G(\omega^* + Lap(\frac{\Delta f}{\epsilon})) \quad (20)$$

289 Finally, use the de-identify human face image to swap the original human face image. In this step,
 290 we use Dlib, which is a toolbox in Opencv based on key-point face detection, to get the 68 key points of
 291 the human faces and use seamless cloning to swap the face. The face swapping algorithm can transfer
 292 the input face features to the target face without obtrusive. An example result is shown in Fig.5 (d).
 293 Intuitively speaking, a larger Laplace noise leads to a more different human face compared with the
 294 original human face.

295 In our experiments, we use Laplace noise parameter ϵ to control the distance between de-identify
 296 human face images and private human face images. In addition, we use the open-source "face
 297 recognition" platform to determine if the synthetic face and the original face represent the same person.

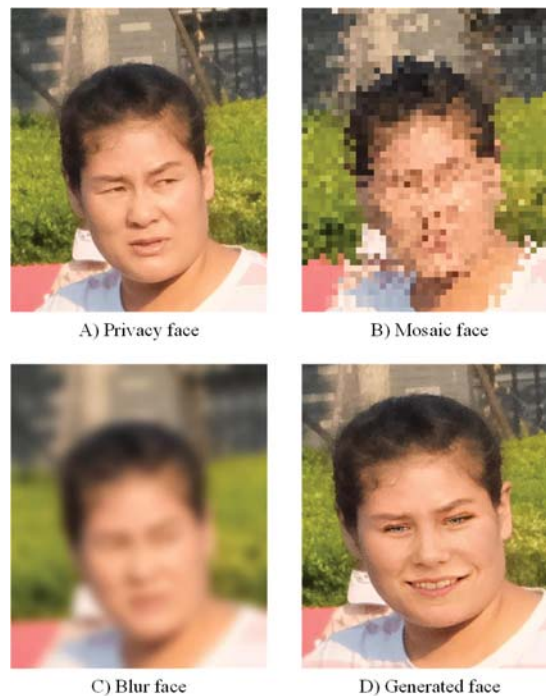


Figure 5. Face images comparison: A) Face in street view, B) Mosaic methods, C) Blur method, D) Our method

298 Fig.5 shows the original private face, the mosaic face, the blurred face, the the new face generated
 299 by StyleGAN. It can be seen that it is not easy for both human and machine to recognize the de-identify
 300 generated face image Fig.5 D as Fig.5 A.

301 5.3.2. Car license plate privacy protection

302 The car license plates are another kind of sensitive objects of IoMT images. As for the privacy
 303 protection of the car license plates, we use Chinese car license plates as our experimental objects. The
 304 car plate should be generated according to the rules enforced by the vehicle management authority. The
 305 rules of a valid Chinese car license plate are: 1) the first character is a Chinese character, representing a
 306 province; 2) the second symbol is an English letter; 3) the last five symbols forms a random string of
 307 letters and numbers, and 4) the background of a license plate is dark blue.

308 After getting the car license plates images from the street images, we use OCR to recognize
 309 the characters and symbols of the car license plates, and then map the car plate into a sequence
 310 of numbers. According to the Chinese car plate rules, the first character will be one of 31 Chinese
 311 province abbreviation characters (except special district). Because of the first Chinese character
 312 represents location information, we map them into 2-digit numbers 00-30 based on the sorted distances
 313 from each province to the capital city Beijing. The mapping table for the first character is shown in
 314 Table ??.

315 Next, the numerical values 0-9 will be translated into 2-digit codes 00-09, and the English symbols
 316 will be translated into 2-digit codes 10-33. For example, a car plate "Beijing A132B3" will be mapped
 317 to a sequence of numbers "00 100103021103". After we translate each car plate into a sequence of
 318 numbers, we add Laplace noise onto the number sequence and obtain a synthetic number sequence
 319 satisfying DP. In Laplace noise generate, we let the $\Delta f = 1$ and control the ϵ to generate the Laplace
 320 noise. For example, if we add a random Laplace noise on the above car plate "00 100103021103", and
 321 obtain a perturbed sequence as "03 130214231502", which can be translated to a synthetic car plate
 322 "Hebei D2ENF2". The above example is illustrated in Fig.6. And there is a cyclic shifting if the Laplace
 323 noise makes the value out of the bounds, e.g. the province code > 33 .

324 Then, we use the generator to generate a synthetic car plate image according to the car plate code.
 325 Finally, we swap the car plate with the synthetic car plate image. The synthetic car plate is protected
 326 by the DP criterion.

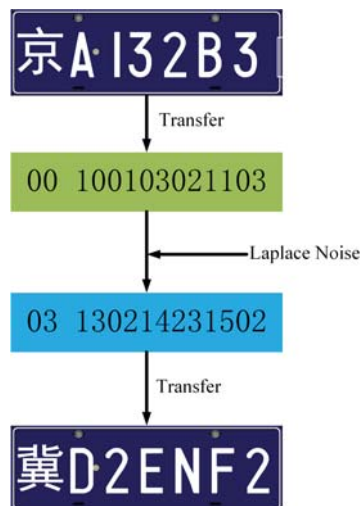


Figure 6. A new car plate content created by DP

327 In the car number transfer, the larger the noise, the longer distance(original car number as origin)
 328 car number will be generated. For example, if a province name is Jilin in a car plate, the province codes
 329 should be generated for Jilin based on the distance from the other provinces to Jilin.

330 Our method uses the synthetic DP car plate to protect the private car plate information. As shown
 331 in Fig. 7, we can see that the car plate is smoothly replaced by our the synthetic car plate.



Figure 7. A typical Chinese car plate swap to protect the street view image

332 It is very important to note that the replacement of the privacy content in a image is not simply a
 333 copy-and-paste job. Instead, it needs to transform the synthetic content by generator into an image
 334 that fits into the original image area with a correct orientation.

335 Therefore, the synthetic image is generally not perceptible to human eyes.

336 5.4. Performance Evaluation

337 5.4.1. Privacy protection metrics

338 In this part, we calculate the distance between the original private image and protected image to
 339 measure the degree of privacy protection.

340 In human face, the average facial distance between the same person is 0.12, which confidence
 341 score is 88. After using our method processed, the average facial distance is 0.45 and confidence
 342 score is 55, which is over the threshold of confidence score 70. This experiment result means our method can
 343 remove the identity of the human face, which means our method can protect the privacy of the human
 344 face image.

345 In car license plate, because of the license plates are strings, their distances are integers. In the
 346 experiment, the distance between the same license plate is 0. After using our method processed,
 347 the distance is 3, which we can consider that the sensitive information of the license plate is protected.

348 5.4.2. Image utility metrics

349 In this part, we set an automatic evaluate module to calculate the degree of image modification
 350 by different metrics through L_0 , L_2 , ALD_p , $SSIM$, and $Dhash$. We compare our method with the Blur
 351 and Mosaic methods. As shown in Fig 8, the Blur and Mosaic remove the sensitive area of privacy.

352 However, a human can easily notice the blur and mosaic in the image. Hence, the computer can easily
 353 recover the information from the processed image.[38][39][40]

354 In our method, we control the generator to generate the de-identify content image with DP
 355 Laplace noise. The de-identify images make both human eyes and computer vision detection methods
 356 not easily to see the difference and get the privacy information on sensitive private objects. The result
 357 of the street view image shown in Fig. 8, as we can see, human and computer can easily detect the
 358 sensitive information in unprotected street view image in Fig. 8 A). And in Fig. 8 B) and 8 C), the
 359 algorithm can not detect the face and the car plate after being blurred, but human can easily see
 360 there are blur or mosaic in the image. In Fig.8 D), the computer algorithm and human detect the fake
 361 sensitive information which had already swapped by our method, so both human and computer can
 362 not get the real sensitive information of the face and the car plate. The privacy in the image is protected
 363 under our method.

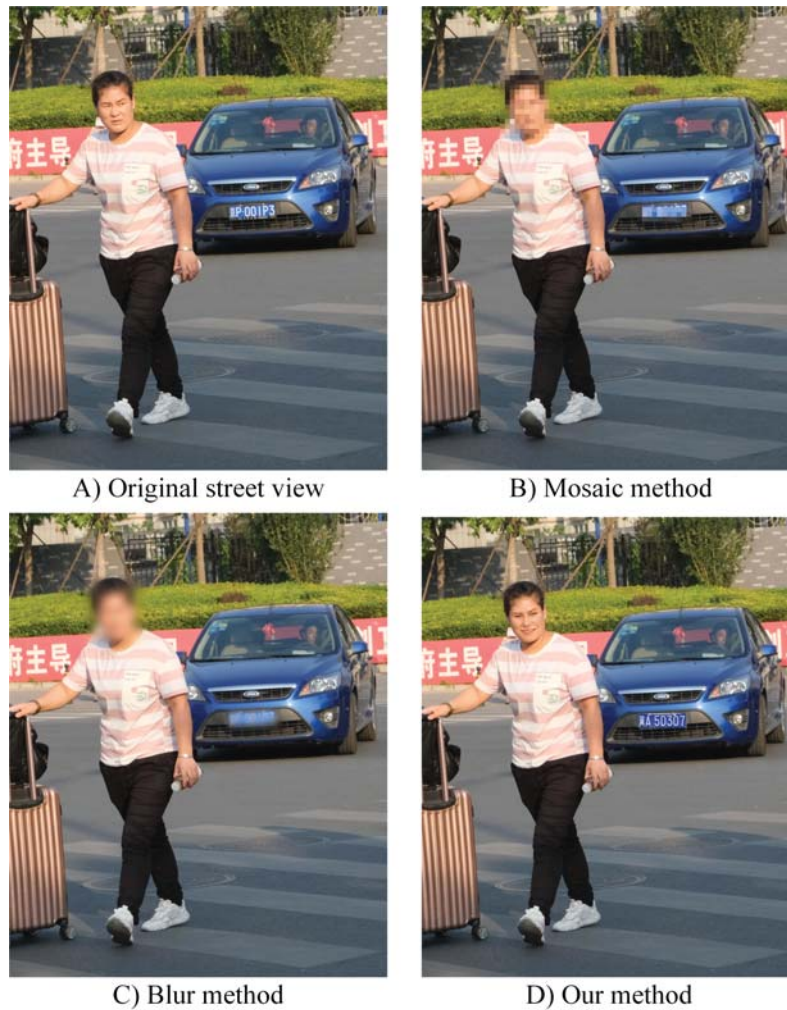


Figure 8. The result of 4 street view image: A) unprotected image, B) image processed with blur, C) image processed with mosaic, D) image processed with our method

364 Next, we use metrics to evaluate the efforts of our methods. Table 1 shows the performance of
 365 our method, blur, and mosaic. The metrics are DHash, SSIM, L_0 , L_2 and ALD_p . The blur and Mosaic
 366 have been modified to change the sensitive area in our experiment images.

367 First, compared with other methods, our methods change the minim pixels to protect the privacy
 368 part of the image. In Dhash, Our method is better than the others. Compared with blur and mosaic,
 369 our method decreases 95.02% and 95.2%. In SSIM, our method is better than others in 1.17% and 1.67%.

370 In L_0 , Our method decreases 73.6% and 72.97%. In L_2 , 86.25% and 25.99%. In ALD_p , our method is
 371 higher than blur and mosaic, which is 160.65% and 98.85%. It is shown that our method is better than
 372 the other two methods in the SSIM, Dhash and L_0 . However, the results show that in the L_2 and ALD_p ,
 373 our method is not the best. After analysis, we found that the L_2 and ALD_p are more suitable in big
 374 area modification. These metrics are not sensitive to minor modifications. So we use the face swap as
 375 an example to show the metrics in the minor modification in a small area. So we choose 89 face swap
 376 images to analysis, the result shows in Table 2. In Dhash, compared with blur and mosaic decreases
 377 96.68% and 96.97%. In SSIM, increase 50.67% and 102.24%. In the L_0 , decrease 76.55% and 76.84%. In
 378 L_2 , decrease 64.93% and 81.08%. In ALD_p , decrease 65.11% and 79.68%. As we can see, our method is
 379 the best in all metrics.

Table 1. Average result of 4000 images with the metrics: Dhash, SSIM, L_0 , L_2 , ALD_p

Methods	Original	Blur	Mosaic	Our methods
Dhash	0	12873.65	13370.19	641.71
SSIM(10^{-2})	100	98.18	97.70	99.33
$L_0(10^2)$	0	1692.25	1652.57	446.74
L_2	0	9983.06	14757.19	18593.41
$ALD_p(10^{-2})$	0	3.99	5.23	10.4

380 6. Conclusion

381 This paper proposes a new image privacy protection method based on GAN and DP. Our method
 382 can protect the sensitive private information contained in the images of IoMT. We use the deep neural
 383 network to identify the private data in the images and de-identified it with the GAN-based content.
 384 Compared with traditional blur or mosaic methods, the proposed method can protect the sensitive
 385 information of image data, avoid the privacy leakage. The experimental results of IoMT collection
 386 image data show that our privacy protection method can protect the privacy with high efficient and
 387 controlability. In future work, we will study the privacy protection on video of IoMT and improve the
 388 real-time nature of our method. Propose high effectively privacy protection method for the privacy of
 389 IoMT.

390 Appendix A.

391 Appendix A.1.

392 References

- 393 1. EU. The EU General Data Protection Regulation . <https://eugdpr.org/>, 2019. [Online; accessed
 394 19-July-2019].
- 395 2. EU. What is considered personal data? <https://gdpr.eu/eu-gdpr-personal-data/>, 2019. [Online; accessed
 396 19-July-2019].
- 397 3. Mannan, M.; van Oorschot, P.C. Privacy-enhanced sharing of personal content on the web. Proceeding of
 398 the 17th international conference on World Wide Web - WWW '08; ACM Press: Beijing, China, 2008; p. 487.
 399 doi:10.1145/1367497.1367564.

Table 2. Average result of 4000 face images with the metrics: Dhash, SSIM, L_0 , L_2 , ALD_p

Methods	Original	Blur	Mosaic	Our methods
Dhash	0	4047.80	4427.79	134.25
SSIM(10^{-2})	100	64.63	48.15	97.38
$L_0(10^2)$	0	1009.4	1022.25	236.72
L_2	0	5832.96	10812.2	2045.48
$ALD_p(10^{-2})$	0	16.68	28.64	5.82

Table A1. The transfer 2-digit code based on distance between Beijing and each province of China

Province Name	Distance to Beijing (km)	2-digit code
Beijing	0	00
Tianjin	96.07188	01
Hebei	239.4603	02
Shandong	356.9375	03
Shanxi	407.3106	04
Neimengu	424.5428	05
Henan	620.2232	06
Liaoning	630.724	07
Jiangsu	860.7032	08
Jilin	867.213	09
Ningxia	884.2019	10
Anhui	897.8403	11
Shanxi	907.8513	12
Hubei	1041.318	13
Shanghai	1041.987	14
Heilongjiang	1056.846	15
Zhejiang	1102.843	16
Gansu	1184.73	17
Jiangxi	1242.833	18
Hunan	1316.041	19
Qinghai	1340.82	20
Chongqing	1419.309	21
Sichuan	1505.931	22
Fujian	1527.525	23
Guizhou	1729.627	24
Guangdong	1856.641	25
Guangxi	2047.263	26
Yunnan	2068.306	27
Hainan	2249.545	28
Xinjiang	2433.955	29
Xizang	2559.149	30

- 400 4. Vyas, N.; Squicciarini, A.C.; Chang, C.C.; Yao, D. Towards automatic privacy management in Web 2.0 with
401 semantic analysis on annotations. Proceedings of the 5th International ICST Conference on Collaborative
402 Computing: Networking, Applications, Worksharing; IEEE: Crystal City, Washington DC, USA, 2009.
403 doi:10.4108/ICST.COLLABORATECOM2009.8340.
- 404 5. Wang, N.; Xu, H.; Grossklags, J. Third-party apps on Facebook: privacy and the illusion of
405 control. Proceedings of the 5th ACM Symposium on Computer Human Interaction for Management
406 of Information Technology - CHIMIT '11; ACM Press: Cambridge, Massachusetts, 2011; pp. 1–10.
407 doi:10.1145/2076444.2076448.
- 408 6. Squicciarini, A.C.; Xu, H.; Zhang, X.L. CoPE: Enabling collaborative privacy management in online
409 social networks. *Journal of the American Society for Information Science and Technology* **2011**, pp. n/a–n/a.
410 doi:10.1002/asi.21473.
- 411 7. Viola, P.; Jones, M.J. Robust real-time face detection. *International journal of computer vision* **2004**, *57*, 137–154.
- 412 8. Tonge, A.; Caragea, C. Image privacy prediction using deep neural networks. *ACM Transactions on the Web*
413 *(TWEB)* **2020**, *14*, 1–32.
- 414 9. Yu, J.; Zhang, B.; Kuang, Z.; Lin, D.; Fan, J. iPrivacy: Image Privacy Protection by Identifying Sensitive
415 Objects via Deep Multi-Task Learning. *IEEE Transactions on Information Forensics and Security* **2017**,
416 *12*, 1005–1016. doi:10.1109/TIFS.2016.2636090.
- 417 10. Uittenbogaard, R.; Sebastian, C.; Vijverberg, J.; Boom, B.; Gavrilă, D.; others. Privacy Protection in
418 Street-View Panoramas Using Depth and Multi-View Imagery. 2019 IEEE/CVF Conference on Computer
419 Vision and Pattern Recognition (CVPR), 2019, pp. 10573–10582.
- 420 11. Liu, Y.; Zhang, W.; Yu, N. Protecting Privacy in Shared Photos via Adversarial Examples Based Stealth.
421 *Security and Communication Networks* **2017**, *2017*, 1–15. doi:10.1155/2017/1897438.
- 422 12. Liu, B.; Xiong, J.; Wu, Y.; Ding, M.; Wu, C.M. Protecting Multimedia Privacy from Both Humans and AI.
423 2019 IEEE International Symposium on Broadband Multimedia Systems and Broadcasting (BMSB). IEEE,
424 2019, pp. 1–6.
- 425 13. Liu, B.; Ding, M.; Zhu, T.; Xiang, Y.; Zhou, W. Adversaries or allies? Privacy and deep learning in big data
426 era. *Concurrency and Computation: Practice and Experience* **2019**, *31*, e5102.
- 427 14. Xue, H.; Liu, B.; Ding, M.; Song, L.; Zhu, T. Hiding Private Information in Images From AI. 2020 IEEE
428 International Conference on Communications (ICC). IEEE, 2020.
- 429 15. McPherson, R.; Shokri, R.; Shmatikov, V. Defeating image obfuscation with deep learning. *arXiv preprint*
430 *arXiv:1609.00408* **2016**.
- 431 16. Pesce, J.P.; Casas, D.L. Privacy Attacks in Social Media Using Photo Tagging Networks: A Case Study with
432 Facebook. p. 8.
- 433 17. Times, T.N.Y. San Francisco Bans Facial Recognition Technology. <https://www.nytimes.com/2019/05/14/us/facial-recognition-ban-san-francisco.html>, 2019. [Online; accessed 19-July-2019].
- 434 18. Girshick, R.; Donahue, J.; Darrell, T.; Malik, J. Rich Feature Hierarchies for Accurate Object Detection
435 and Semantic Segmentation. 2014 IEEE Conference on Computer Vision and Pattern Recognition; IEEE:
436 Columbus, OH, USA, 2014; pp. 580–587. doi:10.1109/CVPR.2014.81.
- 437 19. Hariharan, B.; Arbelaez, P.; Girshick, R.; Malik, J. Hypercolumns for object segmentation and fine-grained
438 localization. 2015 IEEE Conference on Computer Vision and Pattern Recognition (CVPR); IEEE: Boston,
439 MA, USA, 2015; pp. 447–456. doi:10.1109/CVPR.2015.7298642.
- 440 20. Girshick, R. Fast R-CNN. 2015 IEEE International Conference on Computer Vision (ICCV). IEEE, 2015, pp.
441 1440–1448.
- 442 21. Ren, S.; He, K.; Girshick, R.; Sun, J. Faster r-cnn: Towards real-time object detection with region proposal
443 networks. *Advances in neural information processing systems*, 2015, pp. 91–99.
- 444 22. Long, J.; Shelhamer, E.; Darrell, T. Fully Convolutional Networks for Semantic Segmentation. p. 10.
- 445 23. He, K.; Gkioxari, G.; Dollar, P.; Girshick, R. Mask R-CNN. 2017 IEEE International Conference on Computer
446 Vision (ICCV), 2017, pp. 2980–2988.
- 447 24. Efros, A.; Leung, T. Texture synthesis by non-parametric sampling. Proceedings of the Seventh
448 IEEE International Conference on Computer Vision; IEEE: Kerkyra, Greece, 1999; pp. 1033–1038 vol.2.
449 doi:10.1109/ICCV.1999.790383.
- 450 25. Barnes, C.; Shechtman, E.; Finkelstein, A.; Goldman, D.B. PatchMatch: A Randomized Correspondence
451 Algorithm for Structural Image Editing. p. 10.
- 452

- 453 26. Pnevmatikakis, E.A.; Maragos, P. An inpainting system for automatic image structure - texture restoration
454 with text removal. 2008 15th IEEE International Conference on Image Processing; IEEE: San Diego, CA,
455 USA, 2008; pp. 2616–2619. doi:10.1109/ICIP.2008.4712330.
- 456 27. Bertalmio, M.; Vese, L.; Sapiro, G.; Osher, S. Simultaneous Structure and Texture Image Inpainting. *IEEE*
457 *Computer Society Conference on Computer Vision and Pattern Recognition* **2003**, p. 6.
- 458 28. Goodfellow, I.J.; Pouget-Abadie, J.; Mirza, M.; Xu, B.; Warde-Farley, D.; Ozair, S.; Courville, A.; Bengio, Y.
459 Generative Adversarial Networks. *arXiv:1406.2661 [cs, stat]* **2014**. arXiv: 1406.2661.
- 460 29. Klambauer, G.; Unterthiner, T.; Mayr, A.; Hochreiter, S. Self-normalizing neural networks. *Advances in*
461 *neural information processing systems*, 2017, pp. 971–980.
- 462 30. Mao, X.; Li, Q.; Xie, H.; Lau, R.; Wang, Z.; Smolley, S. Least Squares Generative Adversarial Networks.
463 2017 IEEE International Conference on Computer Vision (ICCV), 2017, pp. 2813–2821.
- 464 31. Xiong, W.; Yu, J.; Lin, Z.; Yang, J.; Lu, X.; Barnes, C.; Luo, J. Foreground-Aware Image Inpainting. 2019
465 IEEE/CVF Conference on Computer Vision and Pattern Recognition (CVPR). IEEE, 2019, pp. 5833–5841.
- 466 32. Gulrajani, I.; Ahmed, F.; Arjovsky, M.; Dumoulin, V.; Courville, A.C. Improved training of wasserstein
467 gans. *Advances in neural information processing systems*, 2017, pp. 5767–5777.
- 468 33. Karras, T.; Laine, S.; Aila, T. A Style-Based Generator Architecture for Generative Adversarial Networks.
469 2019 IEEE/CVF Conference on Computer Vision and Pattern Recognition (CVPR). IEEE, 2019, pp.
470 4396–4405.
- 471 34. Sweeney, L. k-anonymity: A model for protecting privacy. *International Journal of Uncertainty, Fuzziness and*
472 *Knowledge-Based Systems* **2002**, *10*, 557–570.
- 473 35. Machanavajjhala, A.; Kifer, D.; Gehrke, J.; Venkatasubramanian, M. l-diversity: Privacy beyond
474 k-anonymity. *ACM Transactions on Knowledge Discovery from Data (TKDD)* **2007**, *1*, 3–es.
- 475 36. Li, N.; Li, T.; Venkatasubramanian, S. t-closeness: Privacy beyond k-anonymity and l-diversity. 2007 IEEE
476 23rd International Conference on Data Engineering. IEEE, 2007, pp. 106–115.
- 477 37. Dwork, C. Differential privacy. *Proceedings of the 33rd international conference on Automata, Languages*
478 *and Programming-Volume Part II*. Springer-Verlag, 2006, pp. 1–12.
- 479 38. Kupyn, O.; Budzan, V.; Mykhailych, M.; Mishkin, D.; Matas, J. DeblurGAN: Blind Motion Deblurring
480 Using Conditional Adversarial Networks. 2018 IEEE/CVF Conference on Computer Vision and Pattern
481 Recognition (CVPR), 2018, pp. 8183–8192.
- 482 39. Nah, S.; Kim, T.H.; Lee, K.M. Deep Multi-scale Convolutional Neural Network for Dynamic Scene
483 Deblurring. 2017 IEEE Conference on Computer Vision and Pattern Recognition (CVPR). IEEE, 2017, pp.
484 257–265.
- 485 40. Menon, S.; Damian, A.; Hu, S.; Ravi, N.; Rudin, C. PULSE: Self-Supervised Photo Upsampling via Latent
486 Space Exploration of Generative Models. *Proceedings of the IEEE/CVF Conference on Computer Vision*
487 *and Pattern Recognition*, 2020, pp. 2437–2445.